

Mitigation of Divertor Heat Loads by Strike Point Sweeping in High Power JET Discharges

S A Silburn^{1,*}, G F Matthews¹, C D Challis¹, D Frigione², J P Graves³, M J Mantsinen^{4,5}, E Belonohy^{6,7}, J Hobirk⁸, D Iglesias¹, D L Keeling¹, D King¹, K Kirov¹, M Lennholm⁷, P J Lomas¹, S Moradi⁹, A C C Sips^{6,7}, M Tsalas¹⁰, and JET Contributors¹¹

¹CCFE, Culham Science Centre, Abingdon, OX14 3DB, UK

²Unità Tecnica Fusione - ENEA C. R. Frascati - via E. Fermi 45, 00044 Frascati (Roma), Italy

³EPFL, Swiss Plasma Center (SPC), CH-1015 Lausanne, Switzerland

⁴Barcelona Supercomputing Center, Barcelona, Spain

⁵ICREA, Barcelona, Spain

⁶JET Exploitation Unit, Culham Science Centre, Abingdon OX14 3DB, UK.

⁷European Commission, B-1049 Brussels, Belgium

⁸Max-Planck-Institut für Plasmaphysik, D-85748 Garching, Germany

⁹Fluid and Plasma Dynamics, ULB - Campus Plaine - CP 231 Boulevard du Triomphe, 1050 Bruxelles, Belgium

¹⁰FOM Institute DIFFER, Eindhoven, the Netherlands

¹¹See the author list of “Overview of the JET results in support to ITER” by X. Litaudon et al. to be published in Nuclear Fusion Special issue: overview and summary reports from the 26th Fusion Energy Conference (Kyoto, Japan, 17-22 October 2016)

E-mail: scott.silburn@ukaea.uk

Abstract. Deliberate periodic movement (sweeping) of the high heat flux divertor strike lines in tokamak plasmas can be used to manage the heat fluxes experienced by exhaust handling plasma facing components, by spreading the heat loads over a larger surface area. Sweeping has recently been adopted as a routine part of the main high performance plasma configurations used on JET, and has enabled pulses with 30MW plasma heating power and 10MW radiation to run for 5s without overheating the divertor tiles. We present analysis of the effectiveness of sweeping for divertor temperature control on JET, using infrared camera data and comparison with a simple 2D heat diffusion model. Around 50% reduction in tile temperature rise is obtained with 5.4cm sweeping compared to the un-swept case, and the temperature reduction is found to scale slower than linearly with sweeping amplitude in both experiments and modelling. Compatibility of sweeping with high fusion performance is demonstrated, and effects of sweeping on the Edge-Localised Mode (ELM) behaviour of the plasma are reported and discussed. The prospects of using sweeping in future JET experiments with up to 40MW heating power are investigated using a model validated against existing experimental data.

1. Introduction

The heat fluxes experienced by plasma facing components (PFCs) in the divertor region of tokamaks, where heat and particles are exhausted from the hot magnetically confined plasma, are characterised by high fluxes localised close to the divertor strike lines [1,2], where the exhaust plasma streams along open magnetic field lines on to the material surfaces. Managing these high heat fluxes to stay within the engineering limits of PFCs, while also achieving high power plasma operation, is a key challenge in the design and operation of ITER and DEMO as well as operation of existing high power devices

* To whom any correspondence should be addressed.

with metallic PFCs such as JET with the ITER-like wall[3]. The high heat fluxes are typically localised over lengths much shorter than the size of the divertor target plates[1]. Strike point sweeping: periodic movement of the divertor strike lines along the tile surfaces during the plasma discharge, is a well-known technique to provide heat flux mitigation by spreading the load over a larger surface area. Sweeping is attractive due to its simple, robust principle of operation, and does not require increasing the impurity content of the plasma by gas puffing of extrinsic impurities[4,5,6] or careful optimisation of divertor plasma conditions [7] to achieve the heat load mitigation. Sweeping is a relevant technique looking to future machines and is under investigation for use on DEMO, where it is anticipated that slow transient high heat flux events, e.g. temporary loss of the nominally highly radiative exhaust plasma conditions, could lead to rapid PFC damage without further mitigation[8]. Recent studies[8,9] have shown that during such events sweeping could be used to give increased margin to the critical heat flux of the PFC cooling (the heat flux above which vapour formation inside the cooling pipes renders the cooling ineffective), and/or avoid component damage such as melting due to high surface temperatures. These studies have so far found that sweeping appears to be compatible with implementation and use on DEMO. Since the JET divertor targets are not actively cooled, in this work we do not consider the issue of critical heat flux and concentrate only on control of component surface temperatures.

Reduction of PFC temperatures by sweeping, with little observed effect on the global plasma behaviour, has been demonstrated previously[10,11], however the routine use of sweeping in high fusion yield plasma scenarios has not been explicitly demonstrated. In addition, there has been little quantitative analysis of sweeping experiments reported to verify how the reduction of PFC temperatures varies with sweeping parameters and extrapolates to higher power operation, or whether plasma response to sweeping could reduce its effectiveness.

A major goal of the 2015-16 JET experimental campaigns has been to further the development of high performance plasma scenarios in preparation for future Deuterium-Tritium (DT) operations. Up to 32MW of auxiliary heating power has been available in the most recent JET experimental campaign and the aim has been to develop pulses for future campaigns where up to 40MW is anticipated. The high power combined with long pulse lengths has made it essential to routinely employ divertor heat load mitigation to meet the experimental goals without violating PFC temperature limits. Strike point sweeping has been the primary method adopted for this, due to its observed straightforward compatibility with high performance plasma development. In the present work we focus mainly on sweeping in the JET ‘hybrid’ ELMy H-Mode scenario[12]. This is focused on in preference to the higher plasma current ‘baseline’ scenario because the shape of the baseline plasma, which is necessarily different to enable higher plasma current operation, is less flexible in terms of sweeping configurations and so less comprehensive sweeping data exists. Here we present analysis of the effect of sweeping on tile surface temperatures in these plasmas, including the effects of varying the sweeping frequency, amplitude and position. Compatibility of sweeping with high fusion performance is reported and discussed, and extrapolation validated by existing measurements is used to assess the prospects for sweeping in future high power JET experiments.

2. Methods

2.1 Divertor geometry and sweeping configuration

An example divertor magnetic configuration used in JET hybrid scenario plasmas is illustrated in figure 1(a), which shows scrape-off-layer (SOL) magnetic flux contours in a cross-section of the JET divertor at two times representing the extrema of the strike point positions. Sweeping consists of repeatedly moving between these two configurations linearly in time, i.e. changing the strike point positions with a triangular waveform. The control system for sweeping on JET has been described in detail elsewhere[11], and allows the strike point positions to be swept with minimal change of the main plasma shape.

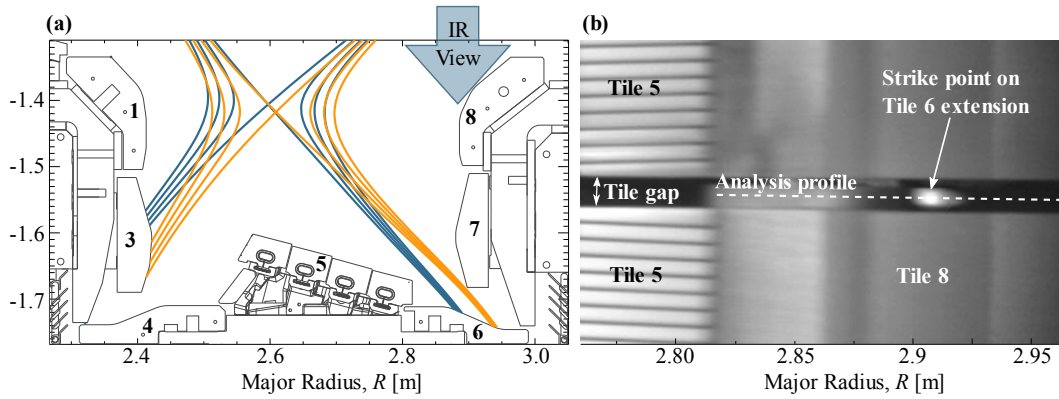


Figure 1: (a) Poloidal cross-section of the JET divertor showing magnetic flux contours at two different times during a pulse with sweeping. JET divertor tile designations are shown by the black numbers on the image and the IR camera viewing direction is indicated. (b) IR camera view of the outboard strike point on the tile 6 extension, showing the line profile used for tile temperature analysis (dashed line).

The outboard strike point (OSP) is placed on the outer horizontal tile row known as tile 6, adjacent to the outboard pumping duct entrance, where the divertor plasma and neutral pumping conditions are known to result in optimal plasma confinement[13,14]. Here we concentrate exclusively on the outer strike point because it is the divertor power handling bottleneck on JET, although it should be noted that both inner and outer strike points sweep synchronously, thus the inner strike point also benefits from the heat load mitigation and could contribute to any effects on plasma conditions related to sweeping. While it is possible to sweep the strike points on JET with large amplitude across multiple tile rows, here we will only consider sweeping with the OSP confined to tile 6. This is desirable to maintain reasonably optimised pumping performance throughout the sweep, rather than suddenly transitioning between neighbouring tiles known to give significantly different divertor conditions and confinement[14]. Tile 6 is made from carbon-fibre composite (CFC) with a $20\mu\text{m}$ thick tungsten coating, and the tile surface temperature is not allowed to exceed 1100°C for longer than 400ms continuously in any given pulse (this is to protect the coating from carbide formation due to the diffusion of carbon from the CFC). The geometry of tile 6 consists of a horizontal section at major radius $R < 2.875\text{m}$, followed by a 24° downward slope towards the outboard side, and another horizontal part from $R > 2.95\text{m}$. With the typical hybrid plasma shape, the strike point position can be placed between approximately $2.85\text{m} \leq R \leq 2.95\text{m}$, although as will be seen in section 3.1 it is not desirable to use this entire range for sweeping.

2.2 Surface Temperature Diagnostics

Surface temperature measurements of tile 6 by high resolution infrared (IR) thermography have been available for the first time in the 2015-16 experimental campaigns. Due to the top-down view of the divertor mid-wavelength IR camera system [15], indicated in figure 1(a), most of tile 6 has historically not been visible to the camera due to the overhanging vertical target tiles (tiles 7 and 8 in Figure 1) blocking the view. In the 2014-15 JET shutdown, a bolted-on extension piece was added to one tile 6 so that the camera can see the extension through a $\sim 12\text{mm}$ toroidal gap between the tiles above. The resulting camera view is shown in figure 1(b). The IR camera signal is taken along the line profile shown in the figure, and is converted to surface temperature based on calibration with an in-vessel heat source[16], and an emissivity of the tungsten-coated surface at $\lambda = 4\mu\text{m}$ of $\varepsilon = 0.15$ at 200°C , increasing linearly with temperature as $d\varepsilon/dT = 1.1 \times 10^{-4} \text{ K}^{-1}$ [17].

2.3 Tile Temperature Model

To establish the expected effectiveness of sweeping against which to compare experiments, and to extrapolate beyond the current dataset, a model for the tile temperature reduction by sweeping is required. For this purpose, we solve the time-dependent 2D heat diffusion equation using a second order central finite difference scheme. The model domain is a simplified tile geometry consisting of an 18cm (radial direction, R) \times 4cm (vertical depth, Z) rectangular slab with thermal properties

corresponding to the CFC used on JET, as illustrated in figure 2. The tungsten coating on the real tiles is not treated in the model, since it is assumed to have low thermal resistance to the bulk and therefore the thermal evolution of the tile will be dominated by the bulk CFC. This behaviour has been confirmed experimentally[18]. Boundary conditions are such that there is no heat conduction out of the edges of the domain, to reflect the fact that the JET tiles are inertially cooled. A heat flux profile representing the swept strike point is then applied to the top surface of the slab. The spatial shape of the heat flux profile is given by an Eich function[1]: exponential decay outboard of the strike point convolved with a Gaussian, and characterised by the e-folding length λ_q and Gaussian width S . This profile shape is kept constant in time, and its position swept along the slab surface with a triangular waveform of constant frequency f_{sweep} and peak-to-peak amplitude L_{sweep} , as illustrated in figure 2. For our purposes, the values of λ_q and S must be chosen to give a profile which approximates the time-average behaviour of the real strike point, including the effects of fast transient strike point movement e.g. wobbling due to normal operation of the plasma vertical stabilisation, and profile shape changes e.g. spreading during Edge-Localised Modes (ELMs). To this end, we use an empirical scaling obtained by fitting Eich functions to time-resolved high resolution IR data from JET ITER-Like Wall pulses, which was developed to predict divertor temperatures for tile protection purposes[19]. This scaling gives λ_q and S , mapped to the outboard midplane, in terms of plasma and engineering parameters:

$$\lambda_q = \min[2, 1.6 \times (I_p^{-0.24} B_T^{0.52} n_e^{-1} P_{\text{SOL}}^{0.023} f_{\text{ELM}}^{0.15}) + 0.006 \sigma_{\text{RF}}] \quad (1)$$

$$S = \min[0.5, 1.6 \times (I_p^{0.74} B_T^{-0.83} n_e^{-0.6} P_{\text{SOL}}^{0.052} f_{\text{ELM}}^{-0.11}) + 0.002 \sigma_{\text{RF}}]. \quad (2)$$

Here S and λ_q are in millimetres, I_p is the plasma current in mega-amperes, B_T is the toroidal magnetic field in Tesla, n_e is the line-integrated electron density in 10^{20}m^{-2} , $P_{\text{SOL}} = P_{\text{heating}} - P_{\text{radiation}}$ is the power exhausted to the divertor in megawatts, f_{ELM} is the ELM frequency in Hz and σ_{RF} is the standard deviation of the measured radial field magnet circuit current in amps. The absolute power density applied to the tile in the model is such that the integral of the profile over the radial direction is proportional to P_{SOL}/L , where L is the strike line length calculated from the major radius and toroidal wetting factor. The constant of proportionality is set such that the modelled temperatures for real pulses are on average consistent with the IR camera data. In experiments it was found that the heat flux to tile 6 abruptly dropped outboard of $R \sim 2.95\text{m}$, at which point the heat load is scraped off

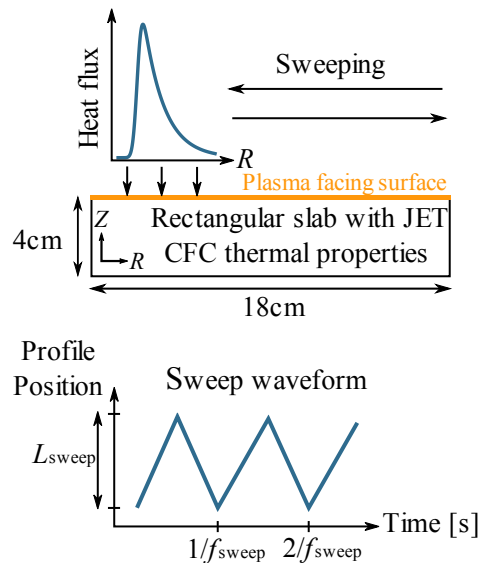


Figure 2: Cartoon illustrating the tile temperature model described in section 2.3.

by the adjacent vertical target (tile 7) rather than reaching tile 6. In the case of the tile 6 extension measured here, this shadow is cast by the vertical target tile toroidally clockwise from the tile gap (bottom of figure 1(b)). To represent this in the model, the applied heat flux at positions equivalent to $R > 2.95\text{m}$ was always forced to zero. The output of this model is the tile surface temperature as a function of major radius and time, which can then be post-processed in the same manner as the IR measurements to compare the two.

3. Results & Discussion

3.1 Tile temperature reduction and effects of sweeping parameters

Figure 3 shows the evolution of the measured tile surface temperature in three hybrid pulses with $I_p = 1.4\text{ MA}$, $B_T = 1.9\text{ T}$ and $P_{\text{SOL}} = P_{\text{heating}} - P_{\text{radiation}} \sim 10.5\text{ MW}$, nominally repeated except for different sweeping configurations: no sweeping, 2cm and 5.4cm sweeping at 4Hz. P_{SOL} is well matched in all 3 pulses for the first 3s of auxiliary heating, as illustrated by P_{heating} and $P_{\text{radiation}}$ plotted in Figure 3(c). The divertor target temperature is measured at major radius $R=2.872\text{m}$, which was the location of the maximum temperature in the un-swept pulse and close to the centre of the sweeping range. The three pulses are only comparable for the first 2.5s of the NBI heating, after which unintentional movement of the strike point in the unswept pulse, and later differences in NBI heating power, create differences in the divertor heat loading. After 2.5s of NBI heating, the pulse without sweeping shows a tile surface temperature rise of around 590°C , compared to 395°C ($\sim 33\%$ reduction) with 2cm sweeping and 280°C ($\sim 52\%$ reduction) for 5.4cm sweeping (the values quoted for the swept pulses are approximate averages over the sweeping cycle). The temperature rise is clearly reduced slower than proportionally with the sweep amplitude, i.e. slower than the reduction in time-averaged heat flux, with a factor 2.7 increase in sweep amplitude resulting in 0.7 times the temperature rise.

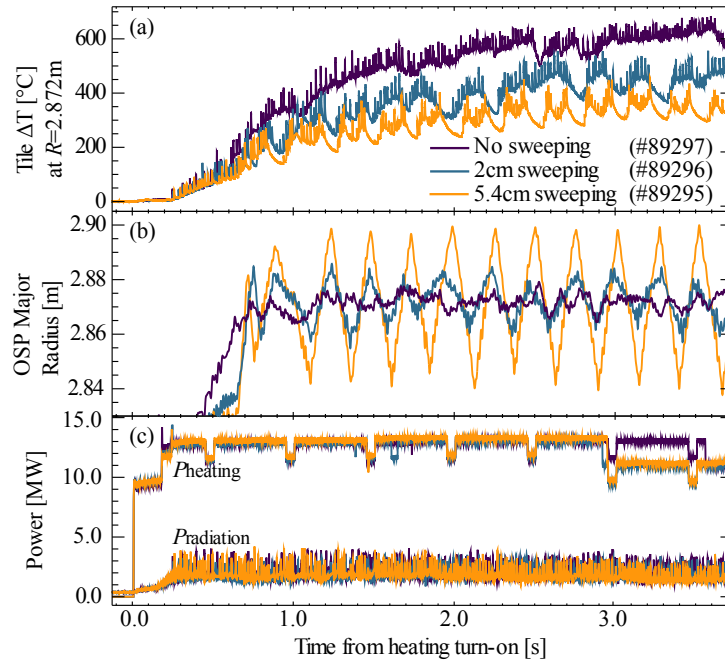


Figure 3: Comparison of pulses with different sweep amplitudes: no sweeping, 2cm and 5.4cm sweeping. (a) Tile surface temperature rise (b) Strike point position (c) Input and radiated power.

Similar behaviour is shown by the model described in section 2.3, as illustrated in figure 4 which shows the modelled scaling of the surface temperature rise and time-averaged heat flux (averaged over 1 sweep cycle) at the sweep centre position, with increasing sweeping amplitude and a similar pulse length and heat flux profile to the real pulses. The 2cm and 5.4cm sweeping pulses above are plotted as points for comparison. The model shows $\sim 30\%$ reduction in temperature rise for 2cm and $\sim 60\%$ reduction for 5.4cm sweeping, similar to the experiment, although the additional benefit from the larger sweeping appears lower in the experiment than the model. This could be related to the un-optimised strike point position in these pulses giving rise to tile geometry effects on the temperature rise, discussed further below, which are not accounted for in the flat slab geometry of the model. In general, in both experiments and model the tile temperature reduction scales slower than might be expected simply from the increasing area of the heat spreading. This highlights that the 2D dynamics of heat diffusion in the tile result in surface temperature behaviour which cannot be well predicted using intuitive time or space-averaged considerations.

An important practical observation during sweeping experiments was the sensitivity of the power handling and sweeping effectiveness to strike point position. Figure 5 shows the surface temperature evolution at $R = 2.86\text{m}$ and $R = 2.90\text{m}$ in the same 5.4cm swept pulse as shown in figure 3 (JET pulse 89295). These locations are approximately equidistant from the ends of the sweep, so ideally would be expected to show similar temperature evolution. It can be seen however that the point at $R = 2.86\text{m}$ (horizontal part of the tile) undergoes temperature cycling of almost 100°C in each sweep period compared to around 40°C at $R = 2.90\text{m}$ (sloped part of the tile), in addition to being around 90°C hotter on average. The deeper temperature cycling is explained primarily by the fact that the angle between the incoming divertor leg and tile surface is $\sim 23^\circ$ larger on the horizontal part of the tile, resulting in a narrower projection of the heat flux profile on to the surface and therefore higher heat flux density. Further analysis is needed to confirm the cause of the higher average temperature, however these observations are enough to motivate avoiding the horizontal part of the tile for sweeping. Based on this, the maximum extent of tile 6 usable for “good” sweeping performance is identified as $R \sim 2.88\text{m} - 2.95\text{m}$ i.e. a maximum sweep amplitude of 7cm.

While the standard sweeping configuration on JET uses $f_{\text{sweep}} = 4\text{Hz}$, some pulses using 8Hz and 20Hz sweeping have also been performed. Although not enough high quality data from well matched pulses were obtained to perform a detailed comparison, similar pulses with different sweep frequencies showed similar overall tile temperature rise, with generally smaller oscillation of the

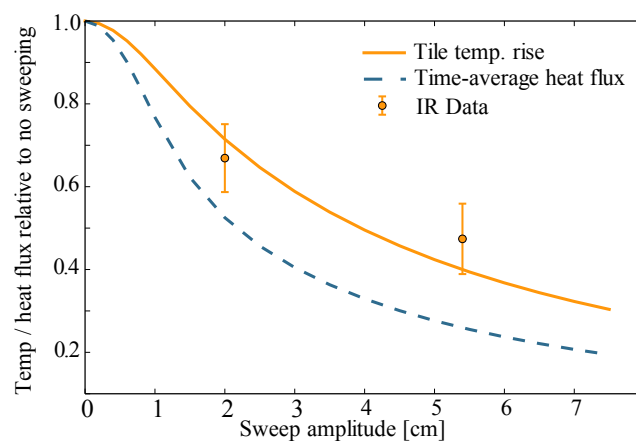


Figure 4: Modelled scaling of tile temperature rise (solid line) and heat flux (dashed line) at the sweep centre position, averaged over 1 sweep period with varying sweep amplitude after 2.5s of sweeping for a pulse similar to pulse 89297. Experimental points from pulses 89295 and 89296 are shown for comparison.

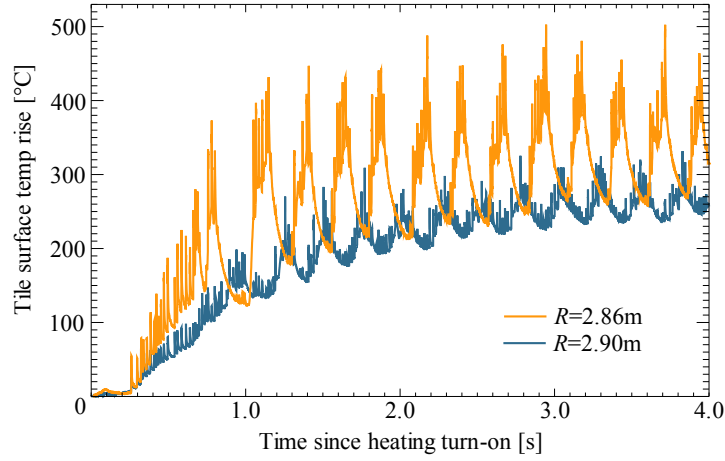


Figure 5: Comparison of measured surface temperature evolution on tile 6 at $R = 2.86\text{m}$ and $R = 2.90\text{m}$ in JET pulse 89295.

(inter-ELM) tile temperature at higher frequencies. This is expected since higher frequencies correspond to each point on the tile receiving shorter and more frequent periods of heating. This is an advantage of higher sweep frequencies already discussed elsewhere[9]: reduction in absolute peak temperature and increase in thermal fatigue lifetime of components compared to lower frequencies due to the less pronounced temperature cycling. Varying the sweeping frequency may also change the degree to which the plasma ELM behaviour is affected by the sweeping, as will be discussed in section 3.2.

To establish whether the tile temperature benefit from sweeping, and its variation with sweep and plasma parameters, is captured by the model described in section 2.3, the temperature rise measured by the IR camera in 21 swept discharges was compared to the model. Pulses with a wide range of parameters were chosen deliberately to highlight any major discrepancies with the scaling, with pulses covering $I_p = 1.8 - 3 \text{ MA}$, $P_{\text{SOL}} = 10 - 21 \text{ MW}$, $L_{\text{Sweep}} = 2.2 - 6.8 \text{ cm}$ and time windows of $1.7 - 7.3 \text{ s}$. Of the pulses used, 15 were hybrid scenario development pulses and a further 5 were baseline scenario development pulses. No pulses or time windows with sweeping on the inboard horizontal part of tile 6 were included. For each pulse, the model was run with the average engineering parameters of the pulse over the time window as inputs, with the time window from the start of the main heating phase until either the end of the strike point sweeping or significant perturbation of the pulse e.g. significant drop in heating power. For both the modelled and experimental temperature data, the maximum surface temperature over the radial direction was extracted at each time point and the temperature just before the auxiliary heating turn on subtracted, to obtain the temperature rise ΔT at each time point. The maximum and minimum of this value during the final sweep cycle were then compared between the model (ΔT_{model}) and inter-ELM IR data ($\Delta T_{\text{measured}}$). The results are shown in figure 6. Good agreement is found between the model and measured temperature rise, with a standard deviation of 55°C for the distribution around $\Delta T_{\text{measured}} = \Delta T_{\text{model}}$ (dashed line in figure 6). This gives confidence that the model captures the scaling of tile 6 temperatures in swept pulses, and can be used for extrapolation to other plasma and sweep parameters.

3.2 Sweeping in high performance hybrid plasmas

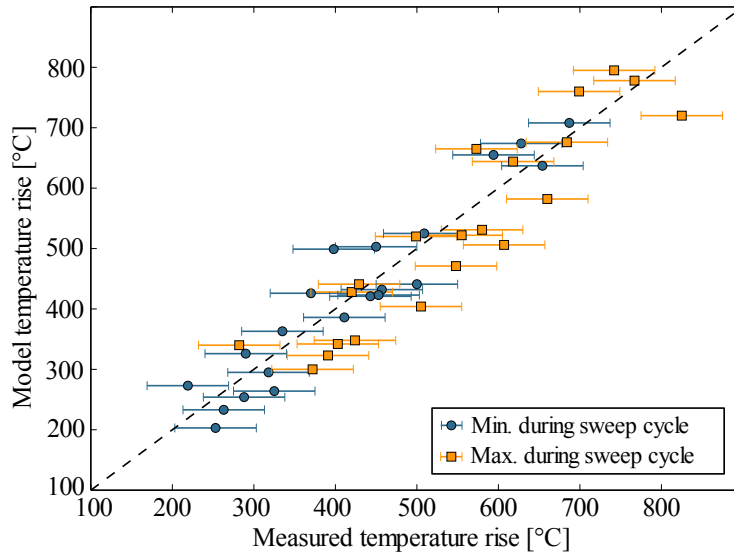


Figure 6: Comparison between measured and modelled tile temperature rise in sweeping pulses. Circles: minimum temperature during sweep cycle, squares: maximum during sweep cycle.

During the 2015-16 experiments, the JET hybrid scenario adopted sweeping with $f_{\text{sweep}} = 4\text{Hz}$ and $L_{\text{sweep}} = 3 - 4\text{cm}$, centred around $R \sim 2.92 - 2.93\text{m}$, as the standard divertor configuration. With this configuration, it was possible to run an $I_p = 2.4\text{MA}$, $B_T = 2.8\text{T}$ hybrid pulse with 30MW total auxiliary heating power (consisting of 25MW NBI and 5MW Ion Cyclotron Resonance heating (ICRH)), 10MW radiation, and a heating duration of 5s without reaching the tile temperature limit (JET pulse 92069). The maximum inter-ELM tile surface temperature measured by the IR camera in this pulse was around 700°C at the end of the heating phase. It should be noted that this sweeping configuration not only spreads the power load on tile 6, but places the divertor leg close enough to the outer vertical target (tile 7) that a significant amount of energy is also scraped off on to the vertical target. This is confirmed by analysis of the tile cool-down after the pulse using embedded thermocouples[20,21], which indicates that in pulse 92069 the vertical target received 27% of the total energy delivered to the divertor, which is very similar to tile 6 itself at 33%. This is compared to a hybrid pulse with similar sweep amplitude but with the sweep centred 3cm further inboard, i.e. with larger clearance to the vertical target, where 55% of the divertor energy was delivered to tile 6 and only 14% to the vertical target. The optimised hybrid sweeping configuration is therefore seen to take advantage of the JET divertor geometry to achieve better power handling than sweeping on a large single tile.

During the 2015-16 experiments, significant progress was made in improving the absolute performance of JET ITER-Like Wall hybrid plasmas, with the best Deuterium-Deuterium fusion neutron yield, averaged over 1 second, improved from $2 \times 10^{16}\text{s}^{-1}$ in 2014 to $2.8 \times 10^{16}\text{s}^{-1}$ in the new experiments. The highest performing pulses from previous campaigns had lower auxiliary heating power than the new highest performing pulses, and did not use sweeping (although non-periodic single slow movements of the strike point were used), while the new higher performing pulses used the sweeping configuration described above. While directly comparable pulses with and without sweeping are not available, this clearly demonstrates that swept divertor configurations can be compatible with access to high fusion performance on JET.

While steady global plasma conditions and performance were achieved in pulses with sweeping, significant modulation of the ELM frequency with the sweeping was sometimes observed. This can be illustrated by taking a coherent average over the sweeping cycle of the instantaneous ELM frequency, i.e. $1/\Delta t$ where Δt is the time between an ELM and its nearest neighbour. Results from a hybrid plasma with $L_{\text{sweep}} = 3\text{cm}$, $f_{\text{sweep}} = 4\text{Hz}$ are shown in figure 7. The ELM frequency is clearly seen to vary synchronously with the sweeping, with the maximum ELM frequency occurring close to the centre position when the strike point is in motion and lower ELM frequency at each end of the sweep. In some pulses a different behaviour was also observed, in which the ELM frequency changed suddenly as the strike point was swept through a position of $R \sim 2.92\text{m}$, with lower frequency ELMs at larger radius. These two distinct behaviours suggest two different effects on the ELM frequency by sweeping: one due to the change in divertor neutral pressure as the pumping efficiency changes during the sweep (giving ELM frequencies dependant on strike point position), and another due to currents driven in the plasma by changing the magnetic configuration (giving ELM frequencies dependant on the rate of change of the magnetic configuration, similarly to ELM triggering by vertical kicks[22]). No significant deleterious effects accompanying the ELM modulation have so far been identified, however it cannot be ruled out that this could change if operating in a different parameter range e.g. with larger amplitude sweeping in the future. Further work is therefore required to quantify and understand the implications of both types of effect on ELM frequency. For example, although the corner configuration is known to give optimal pumping to achieve high confinement compared to having the strike point on other tiles[14], the variation of pumping efficiency and confinement within the range used here for sweeping are not currently well characterised. The most extreme example of ELM synchronisation observed is illustrated in figure 8, which shows the heat flux at the surface of tile 6, inferred from the IR temperature data using the THEODOR code[23], during a test using $f_{\text{sweep}} = 20\text{Hz}$ and $L_{\text{sweep}} \sim 6\text{cm}$. Before the sweeping, regular ELMs at a frequency of 42Hz are observed, but within a single period of the sweeping starting, the ELMs synchronise with the sweeping with 1 ELM occurring at the same point in each sweep cycle, again near the centre position. It is not clear whether, even if such ELM pacing effects could be reliably reproduced, this would represent an advantage or disadvantage for the overall plasma scenario. For example, with the ITER-Like Wall it is necessary to maintain an ELM frequency of typically $>10\text{Hz}$ to prevent excessive radiation from the plasma core due to Tungsten influx [24], and the main actuator used for this is typically gas fuelling[25]. If ELMs could be robustly paced at sufficient frequency by sweeping, it may be possible

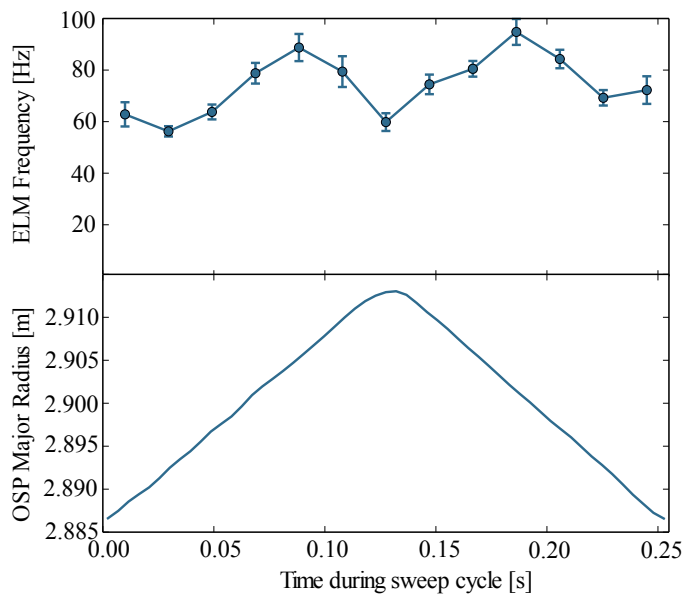


Figure 7: Variation of ELM frequency over the sweep cycle during JET pulse 90271 (3cm, 4Hz sweeping). Top: coherent average of the ELM frequency over 24 sweep cycles. Bottom: strike point major radius.

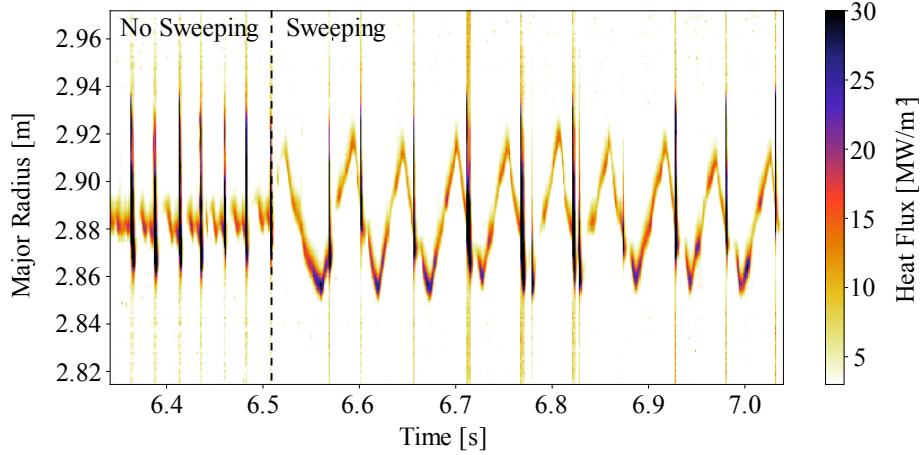


Figure 8: Heat flux on Tile 6 inferred from the IR camera temperatures, as a function of time and major radius, for a 20Hz sweeping test (#92324). Regular 42Hz ELMs are seen before the sweeping starts at just after 6.5s, after which the ELMs quickly synchronise with the sweeping.

to use lower gas fuelling resulting in a lower density, higher performance plasma. On the other hand, in such a situation the ELM heat load would effectively no longer be swept if it arrived at the same point in each sweep cycle, potentially interfering with the efficacy of the sweeping for heat load control.

3.3 Extrapolation to higher input power

Having established sweeping as the routine mode of heat load mitigation in the JET hybrid scenario, an important question is whether it will remain sufficient for future higher power JET campaigns, where up to 40MW of auxiliary heating is expected to be available (~ 33 MW NBI and ~ 7 MW ICRH). To investigate this, the validated tile temperature model was used to estimate the maximum pulse length before reaching the tile 6 temperature limit for different plasma configurations. The case of the existing pulse 92069 is considered as a validation / comparison case, along with two extrapolations to 40MW auxiliary heating power. The two 40MW extrapolations make different assumptions of how the radiated power will scale when increasing the input power: the first assumes that the radiated fraction $F_{\text{rad}} = P_{\text{rad}} / P_{\text{heating}}$ will remain similar to existing pulses at $\sim 1/3$, while the other assumes the absolute radiated power P_{rad} remains similar at ~ 10 MW, i.e. all of the extra input power is exhausted to the divertor. Both the extrapolated cases are based on the existing pulse 92069 with P_{SOL} increased according to the above, and f_{ELM} increased from 30Hz in the existing to pulses to 45Hz, consistent with the observed scaling of ELM frequency with input power in hybrid pulses in the most recent campaigns. In all 3 configurations, the sweep was located such that the outermost point of the sweep was $R = 2.935$ m. For each configuration, the temperature rise model was run with a range of sweep amplitudes, each time until the peak surface temperature remained above 1000°C for 400ms. This is similar to the real protection limit on JET of 1100°C for 400ms, with a lower temperature threshold to allow for known tile-to-tile variations. A starting tile temperature of 160°C was assumed, as typical in existing experiments. The results are shown in figure 9, along with a point representing the actual pulse 92069. As in the experiment, the results show that this pulse was within the pulse length limit expected for its sweeping amplitude and exhausted power. For the 40MW extrapolation cases, the results indicate that a sweeping amplitude between 5.0 – 6.0 cm would be required to stay within the tile temperature limit for a 5s pulse, depending on whether constant F_{rad} or P_{rad} is assumed. Given the available “good” sweeping range of up to 7cm on tile 6 established in section 3.1, these results suggest that running 40MW, 5s hybrid plasmas using tile 6 sweeping may just be possible without having to introduce additional heat load mitigation, e.g by impurity seeding or raising the currently allowed temperature limits.

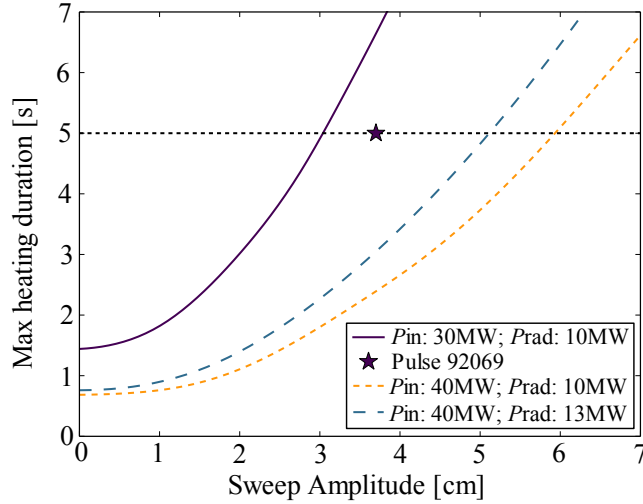


Figure 9: Estimated heating duration before reaching tile 6 temperature limits for $I_p=2.4\text{MA}$, $B_T=2.8\text{T}$ hybrid plasmas with 4Hz sweeping. The three curves indicate the expected pulse length limit for different input power and radiation levels as indicated on the figure. The star represents the longest pulse with $P_{in} = 30\text{MW}$, $P_{rad} = 10\text{MW}$ run during the recent campaigns (#92069). The horizontal dotted line is the desirable pulse length of 5s.

4. Summary

In this work we have presented analysis of the effectiveness of divertor strike point sweeping for PFC heat load mitigation on JET. Strike point sweeping at 4Hz over a distance of 3 – 4cm has been adopted as the standard configuration in the JET ‘hybrid’ high performance ELMy H-Mode scenario, motivated by the need to mitigate divertor heat loads with the $\sim 30\text{MW}$ of input power available in the most recent campaign. The effect of sweeping on the temperature of the outer horizontal ‘tile 6’ has been analysed based on IR camera data, and a model based on an empirical heat flux width scaling and 2D heat diffusion with a simplified tile geometry. A reduction of around 50% in surface temperature rise was observed with 5.4cm sweeping compared to no sweeping, and the temperature reduction with increasing sweep amplitude is slower than linear both in experiment and the model. The JET divertor geometry was found to influence the efficacy of the sweeping significantly, making strike point position an important parameter to optimise. This is due to worse power handling of the outer horizontal target observed at $R < 2.88\text{m}$, and improved power handling at larger R by allowing power to be scraped off to the vertical target. Comparison between modelled and measured divertor temperatures in pulses with a range of plasma and sweeping parameters show that the model appears to capture the general scaling of divertor temperatures with plasma and sweep parameters.

Progress in improving the absolute fusion performance in JET ILW hybrid plasmas while using sweeping has demonstrated that sweeping is compatible with access to high fusion performance. The main side effect of sweeping observed in the plasma is modulation of the ELM frequency, which does not appear to have a significant effect on the global plasma behaviour in typical pulses run in the recent campaigns. With higher frequency 20Hz sweeping, it was found that the ELMs could become strongly synchronised with the sweeping, although it is not yet clear what are the necessary conditions for this behaviour, and whether it could be an advantage or disadvantage to the scenario. Further work is required to better characterise and understand the effect of sweeping on ELMs, pumping, and any related consequences for plasma performance, particularly towards larger sweeping amplitudes which will be required in future. In the recent JET campaigns sweeping has allowed hybrid pulses with 30MW of auxiliary heating and 10MW radiation over 5s pulse lengths to be run without reaching tile temperature limits, in part by taking advantage of the power sharing between multiple tiles due to the strike point positioning.

Based on the tile temperature model validated against pulses in the recent campaigns, the maximum pulse length which could be achieved before reaching tile surface temperature limits has

been estimated for hybrid pulses extrapolated to 40MW heating power. The results suggest that it may just be possible to run 40MW, 5s duration hybrid plasmas using ~6cm sweeping on tile 6 without the need for additional heat flux mitigation techniques or relaxing temperature limitations on the tiles.

It is the decoupling of the divertor heat load mitigation from the plasma conditions achieved thus far which makes sweeping attractive for high fusion performance scenarios in JET. Its predictability is why sweeping has promise for future devices like DEMO. As shown in JET there is no such thing as a completely static strike point[26], and since oscillations in strike point position are inevitable in any real tokamak, it makes sense to optimise the sweeping for maximum mitigation within the engineering constraints of the system.

Acknowledgements

This work has been carried out within the framework of the EUROfusion Consortium and has received funding from the Euratom research and training programme 2014-2018 under grant agreement No 633053. The views and opinions expressed herein do not necessarily reflect those of the European Commission. This work was also part-funded by the RCUK Energy Programme under grant EP/I501045. To obtain further information on the data and models underlying this paper please contact PublicationsManager@ccfe.ac.uk.

References

- [1] Eich T, Sieglin B, Scarabosio A, Fundamenski W, Goldston R. J and Hermann A, 2011 *Phys Rev Lett* 107, 215001
- [2] Eich T et al. 2013 *Nucl Fusion* 53 093031
- [3] Matthews G.F et al. 2011 *Phys. Scr.* 2011 014001
- [4] Giroud C et al. 2013 *Nucl Fusion* 53 113025
- [5] Kallenbach A et al. 2013 *Plasma Phys Contr F* 55 124041
- [6] Telesca G et al. 2016 *Nuclear Materials and Energy* doi:10.1016/j.nme.2016.10.012
- [7] Guillemaut C et al. 2017 *Plasma Phys Contr F* 59 045001
- [8] Maviglia F et al. 2016 *Fusion Eng Des* 109-11 1067
- [9] Li M, Maviglia F, Gianfranco F and Jeong Ha Y 2016 *Fusion Eng Des* 102 50
- [10] Jacquinot J 1995 *Fusion Eng Des* 30 67
- [11] Ambrosino G, Ariola M, De Tommasi G, Pironti A, Sartori F, Joffrin E and Villone F 2008 *IEEE T Plasma Sci* 36 834
- [12] Hobirk J et al. 2012 *Plasma Phys Contr F* 54 095001
- [13] Maggi C et al. 2015 *Nucl Fusion* 55 113031
- [14] E. Joffrin et al. 2017 *Nucl Fusion* 57 086025
- [15] Balboa I et al. 2012 *Rev Sci Instrum* 83 10D530
- [16] Balboa I et al. 2016 *Rev Sci Instrum* 87 11D419
- [17] Ruset C et al. 2017 *Fusion Eng Des* 114 192
- [18] Greuner H, Boswirth B, Eich T, Herrmann, Maier and Sieglin B 2014 *Phys Scripta* T159 014003
- [19] Riccardo V, Matthews G F, Balboa I, Eich T, Iglesias D and Silburn S 2016 “Power footprint definition for JET divertor protection” presented at 22nd International Conference on Plasma Surface Interactions in Controlled Fusion Devices (PSI 22), Rome.
- [20] Matthews G F, Erents S K, Fundamenski W, Ingesson C, Monk R D and Riccardo V 2001 *J Nucl Mater* 290-293 668
- [21] Matthews G F et al, 2016 *Nuclear Materials and Energy* doi:10.1016/j.nme.2016.12.012
- [22] de la Luna E et al. 2015 *Nucl Fusion* 56 026001
- [23] Herrmann A, Junker W, Gunther K, Bosch S, Kaufmann M, Neuhauser J, Pautasso G, Richter Th, Schneide R, and ASDEX Upgrade Team 1995 *Plasma Phys Contr F* 37 17

- [24] Joffrin E et al. 2013 *Nucl Fusion* 54 013011
- [25] Lennholm M et al. 2015 *Nucl Fusion* 55 063004
- [26] Solano E R et al. 2008 *Nucl Fusion* 48 065005